THE JOURNAL OF BIOLOGICAL CHEMISTRY VOL. 287, NO. 25, pp. 21204–21213, June 15, 2012

Inhibition of Lipid Signaling Enzyme Diacylglycerol Kinase ϵ Attenuates Mutant Huntingtin Toxicity*[S]

Received for publication, November 18, 2011, and in revised form, March 26, 2012 Published, JBC Papers in Press, April 16, 2012, DOI 10.1074/jbc.M111.321661

Ningzhe Zhang[‡], Bensheng Li[‡], Ismael Al-Ramahi[§], Xin Cong[‡], Jason M. Held[‡], Eugene Kim[§], Juan Botas[§], Bradford W. Gibson[‡], and Lisa M. Ellerby[‡1]

From the [‡]Buck Institute for Research on Aging, Novato, California 94945 and [§]Jan and Dan Duncan Neurological Research Institute, Texas Children's Hospital, Department of Molecular and Human Genetics, Baylor College of Medicine, Houston, Texas 77030

Background: A chemical screen using a kinase inhibitor library was carried out in a Huntington disease cellular model.
Results: A target kinase, diacylglycerol kinase ϵ, when inhibited blocked mutant huntingtin toxicity.
Conclusion: Inhibition of diacylglycerol kinase ϵ through pharmacological or siRNA knockdown prevents mutant Htt activation of caspase-3 and decreased levels of phosphoinositides.
Significance: Diacylglycerol kinase ϵ is a novel therapeutic target for Huntington disease.

Huntington disease (HD) is a dominantly inherited neurodegenerative disease caused by a polyglutamine expansion in the protein huntingtin (Htt). Striatal and cortical neuronal loss are prominent features of this disease. No disease-modifying treatments have been discovered for HD. To identify new therapeutic targets in HD, we screened a kinase inhibitor library for molecules that block mutant Htt cellular toxicity in a mouse HD striatal cell model, *Hdh*$^{111Q/111Q}$ cells. We found that diacylglycerol kinase (DGK) inhibitor II (R59949) decreased caspase-3/7 activity after serum withdrawal in striatal *Hdh*$^{111Q/111Q}$ cells. In addition, R59949 decreased the accumulation of a 513-amino acid N-terminal Htt fragment processed by caspase-3 and blocked alterations in lipid metabolism during serum withdrawal. To identify the diacylglycerol kinase mediating this effect, we knocked down all four DGK isoforms expressed in the brain (β, γ, ϵ, and ζ) using siRNA. Only the knockdown of the family member, DGKϵ, blocked striatal *Hdh*$^{111Q/111Q}$-mediated toxicity. We also investigated the significance of these findings *in vivo*. First, we found that reduced function of the *Drosophila* DGKϵ homolog significantly improves Htt-induced motor dysfunction in a fly model of HD. In addition, we find that the levels of DGKϵ are increased in the striatum of R6/2 HD transgenic mice when compared with littermate controls. Together, these findings indicate that increased levels of kinase DGKϵ contribute to HD pathogenesis and suggest that reducing its levels or activity is a potential therapy for HD.

Huntington disease (HD)[2] is caused by a polyglutamine expansion in the N terminus of the protein huntingtin (Htt) (1). A pathological change in HD brain is the massive loss of medium spiny neurons in the striatum and loss of neurons in the cortex as the disease progresses. HD results in chorea, dementia, and eventually death. As there is no cure for HD, new therapeutic treatments are clearly needed. Protein kinases are the second most important group of drug targets, after G protein-coupled receptors. The kinase superfamily, whose members are related in the sequence and structure of their catalytic domain, includes CGMC kinases (including cyclin-dependent kinases (CDKs), glycogen synthase kinases (GSK), mitogen-activated protein kinases (MAP kinases), and CDK-like kinases), CaM kinases, serine-threonine kinases, tyrosine kinases, protein kinase A, G, and C families (PKA, PKC, PKG), and others. Because of their key roles in modulating signal transduction and gene transcription, protein kinases are considered to be important potential targets for drug therapy. We therefore evaluated kinase inhibitors in an HD cellular model and identified diacylglycerol kinases (DGKs) in our cellular screen.

DGKs consist of a family of kinases that catalyze the phosphorylation of diacylglycerol (DAG) to produce phosphatidic acid (PA) (2). Both DAG and PA are important intracellular signaling molecules (2). DAG can activate protein kinase C (PKC), Ras guanyl nucleotide-releasing protein (RasGRP), and transient receptor potential channels (3, 4). Transient receptor potential channels mediate store-operated calcium entry into HD medium spiny neurons, and recently, compounds that target these channels have been shown to block HD neurotoxicity (5). There are 10 human DGK isoforms, and each has unique biochemical properties, expression patterns, and subcellular localization. These enzymes have a DAG binding C1 and catalytic domain. DGKϵ is unique in that it has a preference for substrate selection. DGKϵ favors DAG with 1-stearoyl-2-arachidonoyl (18:0, 20:4) acyl chains, which represent the prevalent acyl chain composition in phosphatidylinositol (PI) and

* This work was supported, in whole or in part, by National Institutes of Health Grants NS40251 (to L. M. E.), NS42179 (to J. B.), and CHDI (to L. M. E. and J. B.). Mass spectrometry instrumentation was supported by National Center for Research Resources shared instrumentation Program Grant S10 RR027953 (to B. G.) and the Mass Spectrometry and Imaging Core funded through PL1 AG032118 (to B. G.).
[S] This article contains supplemental Tables 1 and 2 and Figs. 1–8.
[1] To whom correspondence should be addressed: Buck Institute for Research on Aging, 8001 Redwood Blvd., Novato, CA 94945. Tel.: 415-209-2088; Fax: 415-209-2230; E-mail: lellerby@buckinstitute.org.
[2] The abbreviations used are: HD, Huntington disease; DGK, diacylglycerol kinase; DAG, diacylglycerol; PA, phosphatidic acid; PI, phosphatidylinositol; PIP, phosphatidylinositol phosphate; PIP_2, phosphatidylinositol (4, 5)-biphosphate; RT-qPCR, reverse transcription quantitative PCR; MRM, multiple reaction monitoring; WST-8, 5-(2,4-disulfophenyl)-3-(2-methoxy-4-nitrophenyl)-2-(4-nitrophenyl)-2H-tetrazolium inner salt sodium salt WST; WST, water soluble tetrazolium salts.

its derivatives (6). The DGKϵ knock-out mice showed reduced seizure in response to electroconvulsive shock (7). Also, DGKϵ knock-out mice had lower content of PI with 1-stearoyl-2-arachidonoyl acyl chains (8).

Phosphatidylinositol and phosphatidylinositol phosphates (PIPs) have been implicated in the pathological mechanisms of HD. A vesicle-binding assay has shown that Htt binds different forms of PIPs, whereas the mutant Htt bound to a subset of PIPs more strongly than wild type Htt (9). Mutant Htt has also been shown to sensitize the type 1 inositol (1,4,5)-triphosphate receptor in response to inositol (1,4,5)-triphosphate, which is a second messenger derived from phosphatidylinositol (4,5)-biphosphate (PIP_2) (10). When the *C*-terminal fragment of the type 1 inositol (1,4,5)-triphosphate receptor has been introduced to the striatum of a HD model mouse, neuroprotective effects have been observed (11). However, whether the level of 1-stearoyl-2-arachidonoyl PI and PIPs is related directly with mutant Htt-associated neurotoxicity has not been determined.

To identify potential HD therapeutic targets, we screened a kinase inhibitor library in striatal $Hdh^{111Q/111Q}$ mouse HD cell model. The $Hdh^{111Q/111Q}$ cells are immortalized striatal cells derived from a knock-in mouse model that expresses a mutant form of Htt with an expanded polyglutamine tract of 111 repeats (12). This cell line, together with the normal control line $Hdh^{7Q/7Q}$ cells, represents a commonly used mouse HD cell model. Using multiple assays, we identified DGK inhibitor II, also known as R59949, as an effective compound decreasing toxicity associated with mutant Htt. We evaluated whether DGK inhibition affected lipid metabolism in our $Hdh^{111Q/111Q}$ cellular assay. Indeed, DGK inhibition normalizes altered lipid metabolism in this HD cell model. Analysis of the 10 mouse DGK isoforms in striatal cells and tissue suggests that four family members are expressed highly in the striatum. One family member, DGKϵ, prevents cell death when knocked down in $Hdh^{111Q/111Q}$ cells. Correspondingly, partial loss of function of the *Drosophila* homolog of DGKϵ significantly improves Htt-induced motor dysfunction in a fly model of HD *in vivo*. Our work provides novel mechanisms of neurotoxicity from mutant Htt in HD and identifies DGKϵ as a therapeutic target for HD.

EXPERIMENTAL PROCEDURES

Cell Culture—All cell culture reagents were from Invitrogen unless otherwise stated. Striatal $Hdh^{Q7/Q7}$ and $Hdh^{Q111/Q111}$ cells were maintained in DMEM supplemented with 10% FBS at 33 °C. Culture plates were coated with 50 μg/ml rat tail collagen type-I (BD Biosciences) for 1 h at room temperature before immortalized striatal cells were seeded for experiments. For caspase-3/7 activity assay, Biocoat collagen I-coated 96-well plates from BD Biosciences were used. Knocking down DGK genes was achieved by transfecting corresponding Dharmacon siGENOME SMARTpool siRNAs (Thermo Scientific) via Amaxa Nucleofector kit L (Lonza).

Caspase-3/7 Activity Assay—The caspase activity assay was performed with Apo3 HTS kit (Cell Technology). $Hdh^{111Q/111Q}$ cells cultured in 96-well plates were challenged with serum deprivation along with drug treatments. We used the EMD Calbiochem InhibitorSelect™ 96-well protein kinase inhibitor library I (catalog no. 539744). Inhibitors were dissolved in dimethyl sulfoxide, and the final concentration in the treatment well was 20 μM for all kinase inhibitors except phosphatidylinositol 3-kinase γ inhibitor (10 μM for this kinase inhibitor). DGK inhibitor I (R50922) was purchased from EMD Calbiochem. Control cells were treated with 0.2% dimethyl sulfoxide, the same as the kinase inhibitor-treated cells for 24 h. Medium was removed, and 50 μl of 1× lysis buffer was added to each well. After shaking on an orbital shaker at 700 rpm for 5 min, two 10-μl aliquots of lysate were transferred to new 96-well plates for BCA protein concentration measurement, and 70 μl of substrate mix (1× lysis buffer with 1× Apo3 HTS caspase-3/7 detection reagent and 20 mM DTT) was added into the remaining 30 μl of lysate in each well. The plate was briefly shaken at 700 rpm for 30 s before reading. The Fusion-Alpha Universal Microplate Analyzer (PerkinElmer Life Sciences) was used for this fluorescence-based assay (excitation, 485 nm; emission, 530 nm) at 37 °C. For each sample, the protein concentration was measured in duplicate with Pierce BCA protein assay kit (Thermo Scientific). The caspase activity was normalized against protein concentration for each sample.

WST Assay—$Hdh^{111Q/111Q}$ cells were cultured in 96-well plates as described above. Then the medium was removed, and 100 μl 1× WST-8 reagent (Alexis) was added into each well. The cells were incubated for 2 h at 33 °C before absorbance at 450 nm was measured on a SpectraMax 190 plate reader (Molecular Devices).

Western Blotting—$Hdh^{111Q/111Q}$ cells were treated with serum starvation for 24 h in the presence or absence of drugs. Then cells were scraped off, pelleted, and washed once with PBS (Cellgro). Cell pellets were lysed by sonication in mammalian protein extraction reagent (from Thermo Scientific) containing protease inhibitors (one Complete mini tablet per 10 ml of mammalian protein extraction reagent, Roche Applied Science) and 1% phosphatase inhibitor mixture set II (Calbiochem) at 4 °C. Protein concentration was measured with Pierce BCA protein assay kit to ensure equal sample loading. Protein samples (40 μg) were run on 4–12% Bis-Tris gel (Invitrogen) at 200 V for 1 h, transferred to nitrocellulose membrane (Whatman) at constant 20 V for 14 h at 4 °C, probed with anti-Htt (1:500, MAB2166, Millipore), anti-HttNeo513 (1:750, polyclonal generated as described previously (13) Open Biosystems), and anti-GAPDH (1:10,000, Fitzgerald).

Immunocytochemistry—Treated cells on glass coverslips (Bellco Glass) were fixed by 4% paraformaldehyde for 20 min at room temperature. Fixed cells were permeabilized with 0.1% Triton X-100 (Sigma) for 10 min and blocked with 5% donkey serum (Millipore) in PBS for 1 h. Primary antibodies were diluted with 1% BSA (Roche Applied Science) in PBS. The primary antibody (anti-PIP, 1:200 from Echelon) was incubated overnight at 4 °C. After three washes with PBS, the secondary antibody (Alexa Fluor 488-conjugated donkey anti-mouse IgG, 1:1000 from Invitrogen) was added for 1.5 h incubation at room temperature. Coverslips with stained cells were finally mounted with Prolong Gold Antifade reagent with DAPI (Invitrogen) onto glass slides (VWR) for microscopy.

Reverse Transcription Quantitative PCR (RT-qPCR)—Total RNA was isolated from striatal cells or mouse tissue (10.5 weeks) with the RNeasy mini kit (Qiagen) according to the

manufacturer's instructions. The Buck Institute for Research on Aging is an Assessment and Accreditation of Laboratory Animal Care (no. 001213) international accredited institution. All procedures were approved by the Institutional Animal Care and Use Committee (A4213-01). 1 μg of RNA was converted to complementary DNA (cDNA) by using the MessageSensor RT kit (Applied Biosystems). Real time quantitative PCR (qPCR) was performed with Universal Probe Library (UPL from Roche Applied Science) dyes on the LightCycler 480 system (Roche Applied Science). For quantification the threshold cycle C_T of each amplification was determined by the second derivative analysis provided by LightCycler 480 software, and the $2^{-\Delta\Delta CT}$ method was used to determine the relative expression level of each gene normalized against the housekeeping gene β-actin (ActB). The specificity of each pair of primers was tested by comparing to a negative control sample of water. The following primers were used: DGKα, 5′-ctgggcactggaaatgatct-3′ (forward) and 5′-aatctttctcaaattctcaccttcata-3′ (reverse); DGKβ, 5′-agctgaagtttgcaagtcaaga-3′ (forward) and 5′-atttccattgctccttccaa-3′ (reverse); DGKγ, 5′-tgctcctctgtcaccattagg-3′ (forward) and 5′-cagggctctccgtctacttg-3′ (reverse); DGKδ, 5′-gattgccaaggggagaagtc-3′ (forward) and 5′-tgctcaccagcttctcacaa-3′ (reverse); DGKϵ, 5′-gtattctgcaggcagcagtg-3′ (forward) and 5′-gtcttctggcaccaaatgc-3′ (reverse); DGKζ, 5′-gccaggatggcaagtgtc-3′ (forward) and 5′-acgatctccttgctgtggaa-3′ (reverse); DGKη, 5′-acctccctgtgctcaacact-3′ (forward) and 5′-agcaatggaggcagcaag-3′ (reverse); DGKθ, 5′-ccacctctgctcggacttc-3′ (forward) and 5′-atgggacatgaagttgcaga-3′ (reverse); DGKι, 5′-atgacatccatcaggtgcaa-3′ (forward) and 5′-ctgggacagactggggaat-3′ (reverse); DGKκ, 5′-attggctggctgagtcaaat-3′ (forward) and 5′-ttaaactgcgagtgtcagaagc-3′ (reverse). The primer concentration was 400 nM for the qPCR.

Lipid Extraction—Cells in a 15-cm plate were placed on ice and then washed once with ice-cold PBS, scraped in PBS on ice, and centrifuged. The pellet was suspended in 1200 μl of ice-cold 1:1 chloroform ($CHCl_3$)/methanol (MeOH) (14). After vortexing for 1 min to mix, cells were centrifuged, and the supernatant was discarded. To the pellet, 600 μl of 2:1 ice-cold $CHCl_3$/MeOH with 0.25% 12 N hydrochloric acid (HCl) was added followed by 10 min of vortexing at 4 °C. Then, 120 μl of 1 N HCl was added, and the mixture was vortexed for 15 s followed by centrifuge at 3500 rpm for 5 min. The lower phase was collected and dried under the protection of nitrogen. The pellet was redissolved in 200 μl of 1:1 $CHCl_3$/MeOH with 30 mM piperidine before multiple reaction monitoring (MRM)-MS analysis.

Mass Spectrometry Profiling—To profile the lipids in the extracts, samples were first analyzed by MALDI-MS using a vMALDI-LTQ platform (Thermo Scientific) operating in the negative ion mode. Briefly, 1 μl of matrix (2,5-dihydroxybenzoic acid) dissolved in methanol at 10 mg/100 μl) was gently mixed with 1 μl of extracted phospholipid in 1:1 $CHCl_3$/MeOH solution with piperidine, and the mixture was loaded on an MALDI plate specially marked with ImmEdge Hydrophobic Barrier Pen (Vector Laboratories, Inc.). The laser power was adjusted to optimize the MALDI signal, and spectra were acquired over m/z 300–2000.

Mass Spectrometry MRM-MS Analysis—Samples were analyzed by MRM-MS on a 4000 QTRAP hybrid triple quadrupole/linear ion trap mass spectrometer (AB Sciex) equipped with a Turbo IonSpray source in negative ion mode. Lipid samples were introduced by direct infusion using a syringe pump (Mode 11 series, Harvard Apparatus) at a flow rate of 10 μl/min. A total of 18 ion transition pairs from six base phosphoinositides (34:1, 36:1, 36:4, 38:4, 38:5, and 40:6) with one, two, or three phosphate moieties (PI, PIP, and PIP_2) were quantified by MRM-MS. The negatively charged parent ion was used as the Q1 mass, and the diagnostic fragment ion of the dehydrated headgroup was chosen for Q3 (15), which differentiates phosphoinositides with different fatty acid compositions (supplemental Fig. 1). The Q1 m/z, Q3 m/z, dwell time, declustering potential, collision energy, and collision cell exit potential for each transition are listed in supplemental Table 1. Inositol 1,4,5-trisphosphate species were not included in the study due to their extremely low abundance. Data were collected with an ion spray voltage of −4500 V, curtain gas of 10 psi, nebulizer gas of 25 psi, and an interface heater temperature of 600 °C. MRM-MS transitions were acquired and monitored at unit resolution in both Q1 and Q3. Each sample was typically infused for 3–6 min, and each sample was analyzed two times with the average signal of the runs reported. Quantification was performed using Analyst (version 1.5), and each transition was integrated individually. The quantification results were normalized against cell numbers counted by Z1 Coulter Particle Counter (Beckman Coulter).

Drosophila Motor Performance Analysis—Tests were carried out using 15 age-matched virgin females. Animals were placed in an empty vial and tapped down. The number of animals able to climb 9 cm after 15 s was recorded as a percentage of the total. This was repeated 10 consecutive times, and the average of the ten observations was plotted for each day shown in the chart. Two replicates were tested in parallel for each genotype. Animals were raised at 26.5 °C. The nervous system driver line *elav-GAL*^{c155} was obtained from the Bloomington *Drosophila* Stock Center at University of Indiana. The inducible shRNA line targeting the *Drosophila* homolog of DGKϵ (4659GD) was obtained from the Vienna *Drosophila* RNAi Center. NT-Htt128Q animals express an N-terminal Htt fragment comprising exons 1–4 (first 336 amino acids with 128Q polyglutamine expansion) have been described previously (16).

RESULTS

Kinase Inhibitor Library Screening Identifies DGK Inhibitor II as Therapeutic Target for HD—We screened a kinase inhibitor library that contained 80 different inhibitors (see supplemental Table 2) in the mouse *Hdh*$^{111Q/111Q}$ cell model utilizing caspase activity and WST-8 as endpoints during serum withdrawal (Fig. 1). As reported previously, serum withdrawal results in a dramatic increase in caspase activity in *Hdh*$^{111Q/111Q}$ when compared with *Hdh*$^{7Q/7Q}$ cells (13, 17). We found several inhibitors that reduce caspase-3/7 activity when *Hdh*$^{111Q/111Q}$ cells undergo serum withdrawal. These include Akt inhibitor X, PDK1/Akt/Flt dual pathway inhibitor, chelerythrine chloride, DGK inhibitor II, IGF-1R inhibitor II, Lck inhibitor, PDGF RTK inhibitor III, PKCβ II/EGFR inhibitor, rapamycin, SU11652,

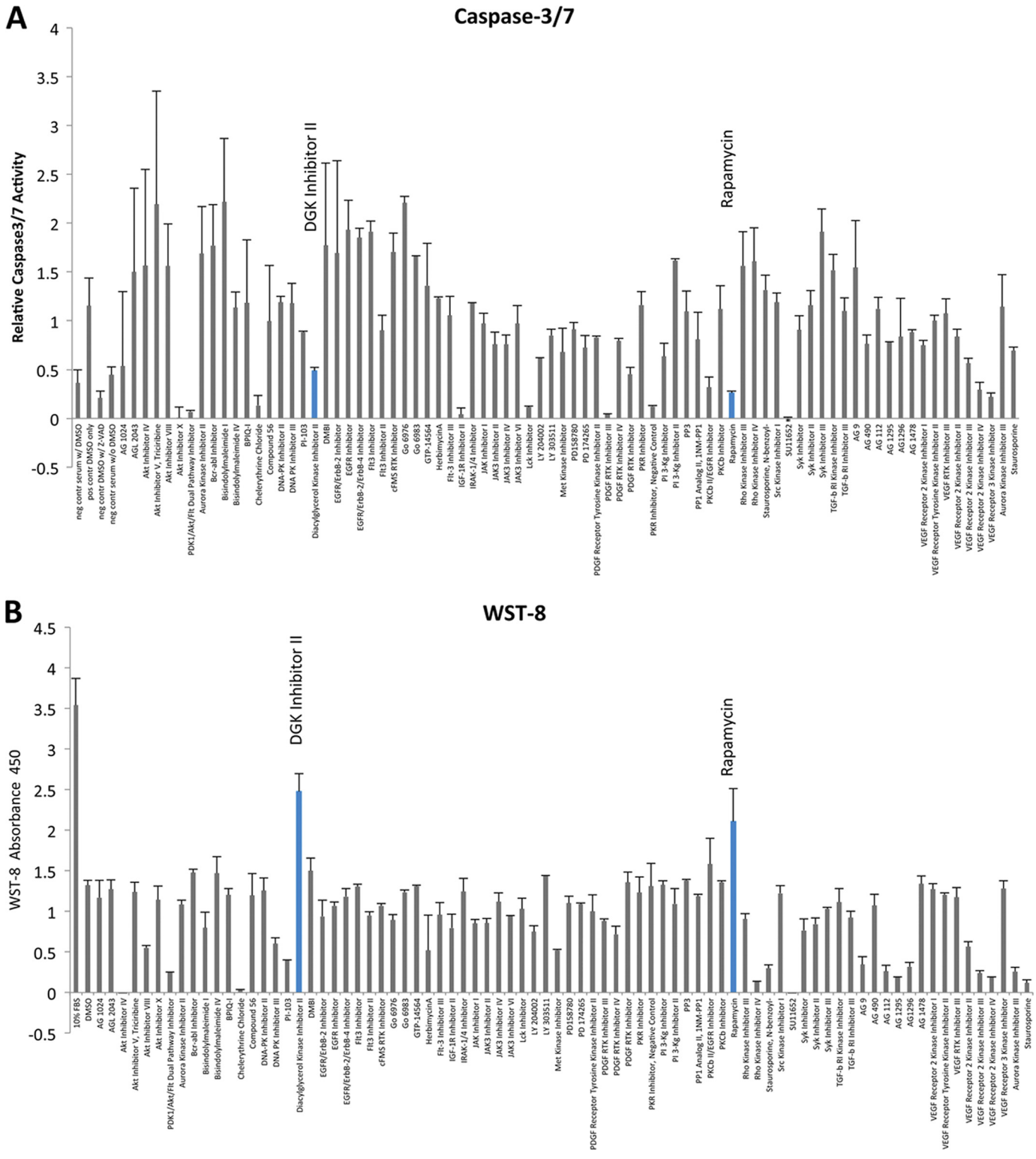

FIGURE 1. **Screening of the kinase inhibitor library identified DGK inhibitor as a potential drug candidate.** *A*, the screening of the kinase inhibitor library in *Hdh*$^{111Q/111Q}$ cells during serum withdrawal using caspase activity assay as an end point. Several kinase inhibitor hits, including DGK inhibitor II, decreased caspase-3/7 activity. *B*, screening the same library using viability WST-8 assay library in *Hdh*$^{111Q/111Q}$ cells during serum withdrawal. The WST-8 assay and caspase activity assay identified DGK inhibitor II along with rapamycin, a known protective molecule, as a hit. See supplemental Table 2 for further details of kinase inhibitors used in this screen. *neg contr*, negative control; *pos contr*, positive control; *DMSO*, dimethyl sulfoxide. The compounds are defined in supplemental Table 2.

VEGF receptor 3 kinase inhibitor, VEGF receptor 2 kinase inhibitor III, and VEGF receptor 2 kinase inhibitor IV (Fig. 1*A*). However, when coupled with WST-8 assay, which measures bioreduction of WST-8 mostly dependent on the glycolytic NAD(P)H production of viable cells, DGK inhibitor II (R59949) and rapamycin were the only kinase inhibitors that protected

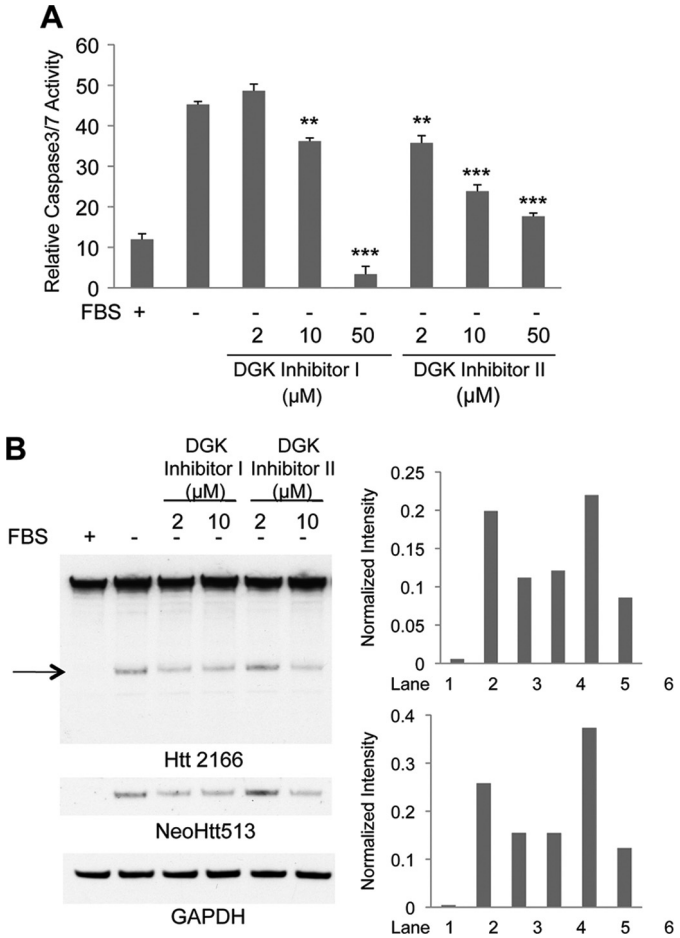

FIGURE 2. **Both DGK inhibitor I (R59022) and II (R59949) reduced caspase activity and mutant Htt proteolysis in *Hdh*$^{111Q/111Q}$ cells undergoing serum withdrawal.** *A*, retesting DGK inhibitor II and the evaluation of related compound DGK inhibitor I confirmed the protective effect of these kinase inhibitors in *Hdh*$^{111Q/111Q}$ cells. We found a dose-dependent reduction of caspase-3/7 activity in *Hdh*$^{111Q/111Q}$ cells after serum withdrawal with DGK inhibitor I and II. DGK inhibitor treatment conditions were compared with FBS withdrawal only condition by one-way analysis of variance (*, $p < 0.05$; **, $p < 0.01$; ***, $p < 0.005$ for all figures). *B*, *Hdh*$^{111Q/111Q}$ cells were treated with different doses of DGK inhibitor I or II during serum starvation. Western analysis demonstrates that serum withdrawal produces huntingtin product detected by Htt 2166 and neoHtt513 antibody, and this fragment was reduced by DGK inhibitors at 10 μM. Control levels of GAPDH suggest equal protein loading. Quantification of the Htt fragment bands was also shown.

Hdh$^{111Q/111Q}$ cells against serum withdrawal (Fig. 1*B*), thus indicating that these compounds act specifically on *Hdh*$^{111Q/111Q}$-induced toxicity. Rapamycin has been reported to reduce HD-associated toxicity through induction of autophagy (18). The identification of DGK inhibitor II as blocking mutant Htt toxicity is novel, and the mechanism of action for this effect is not known. To confirm that other DGK inhibitors were effective in this assay, we tested another DGK inhibitor, DGK inhibitor I (also known as R59022). As shown in Fig. 2*A*, both DGK inhibitors showed reduced caspase activity in a dose-dependent manner, suggesting a role for DGKs in toxicity caused by the polyglutamine mutation in Htt. *Hdh*$^{7Q/7Q}$ cells generally show very modest caspase activation after serum starvation in 24 h, and DGK inhibitors do not alter the caspase-3/7 activity in serum starved *Hdh*$^{7Q/7Q}$ cells (supplemental Fig. 2). Given this result, we utilized *Hdh*$^{111Q/111Q}$ cells for most of our studies.

Mutant Huntingtin Proteolysis Is Reduced in Cells Treated with DGK Inhibitor II—The proteolysis of mutant Htt by caspases to generate the toxic N-terminal fragments is linked directly to the cell death mechanisms in HD. In *Hdh*$^{111Q/111Q}$ cells, proteolysis of Htt was detected upon serum withdrawal (Fig. 2*B*, *lane 2*) using Western blot analysis. Addition of either DGK inhibitor I or II reduced the level of Htt proteolysis (Fig. 2*B*, *lanes 3*, *4*, and *6*). Using an antibody specific to the caspase-3 cleavage site at the 513 amino acid of Htt (NeoHtt513), we found that Htt proteolysis at this site was induced by serum starvation (Fig. 2*B*, *lane 2*) and reduced by treatment with DGK inhibitors (Fig. 2*B*, *lanes 3*, *4*, and *6*). We did not detect cleavage of Htt at amino acids 552 or 586 using neoHtt552 or neoHtt586 under these conditions (data not shown). Immunocytochemistry revealed that cleaved active caspase-3 was induced in *Hdh*$^{111Q/111Q}$ cells upon serum withdrawal (data not shown). Treatment with DGK inhibitor II prevented the generation of cleaved caspase-3 (data not shown).

Protective Effect of DGK Inhibitors in HD Does Not Require PKC—The reaction catalyzed by DGKs is the phosphorylation of DAG into PA. DAG is a well known PKC activator, and the inhibition of DGKs would likely lead to decreased DAG consumption and increased PKC signaling. To test whether this could be the mechanism underlying the protective effects of DGK inhibitors, we treated cells with two PKC inhibitors, bisindolylmaleimide I and Gö6983. Both bisindolylmaleimide I and Gö6983 inhibit PKC isoforms belonging to conventional and novel PKC subfamilies, the two subgroups of PKCs responsive to DAG. Caspase activity, WST-8 and mutant Htt proteolysis were evaluated during serum withdrawal conditions with these two inhibitors. The protective effect achieved by DGK inhibitor II treatment in *Hdh*$^{111Q/111Q}$ cells was not altered by co-treatment of bisindolylmaleimide I or Gö6983 using caspase activity (Fig. 3*A*), WST-8 (Fig. 3*B*) or the proteolysis of Htt (Fig. 3*C*) as end points. DGK inhibitor I did not affect Htt proteolysis in *Hdh*$^{7Q/7Q}$ cells in the presence or absence of PKC inhibitors as expected (supplemental Fig. 3). Both inhibitors showed strong inhibition of PKCs as measured by their effects on phorbol ester-induced PKC activation (data not shown). Therefore, the protective effect of DGK inhibitors on *Hdh*$^{111Q/111Q}$ cells does not require PKC signaling as a downstream mediator.

Altered Phosphoinositides in Hdh$^{111Q/111Q}$ *Cells and DGK Inhibition Normalizes Lipid Metabolism During Serum Withdrawal*—DGKs are critical enzymes involved in lipid metabolism. When certain DGK family members are knocked out in mice, a decrease in polyphosphoinositides is observed (8). Therefore, a critical mechanism for rescue of HD cytotoxicity may be through altered lipid metabolism. Lipid profiling of cellular phosphatidylinositol monophosphate/phosphatidylinolsitol biphosphate (PI/PIP/PIP$_2$) was carried out using mass spectrometry in total extracts from *Hdh*$^{7Q/7Q}$ and *Hdh*$^{111Q/111Q}$. Representative MALDI-MS spectra are shown in supplemental Fig. 4–8. The predominant species is PI, but we were also able to detect PIP and PIP$_2$. We also noted that the distribution and pattern between the *Hdh*$^{7Q/7Q}$ and *Hdh*$^{111Q/111Q}$ extracts is distinct for these lipids (data not shown).

Having established that the PI, PIP, and PIP$_2$ could be detected by MALDI-MS, we quantified the levels in *Hdh*$^{7Q/7Q}$

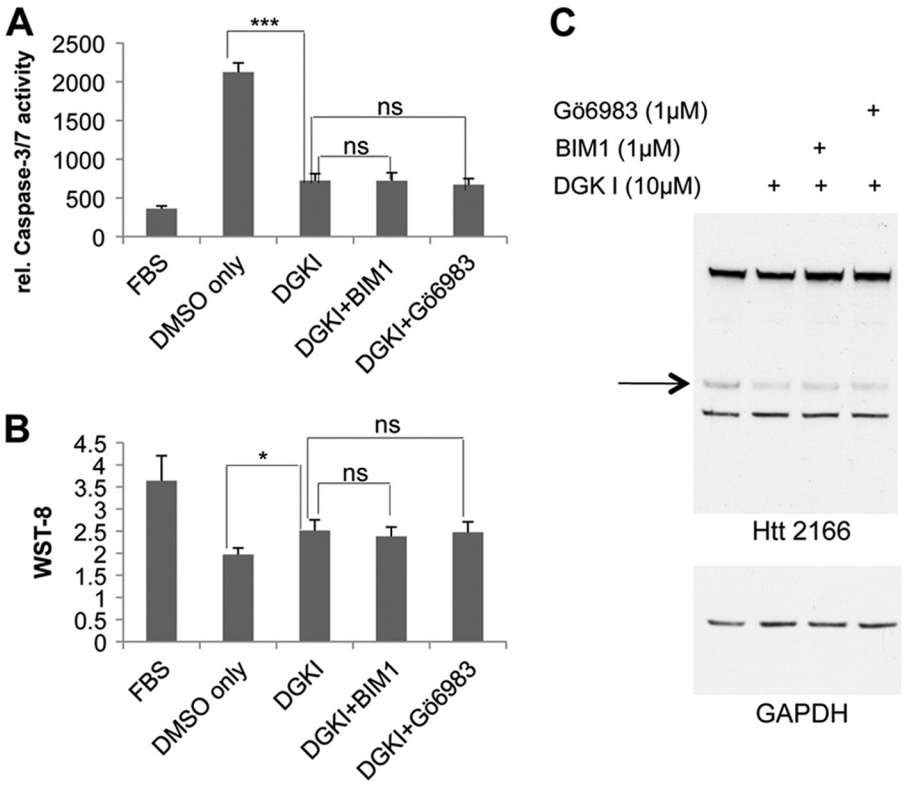

FIGURE 3. **DGK inhibitor did not require PKC to take effects.** *A*, the reduced caspase activity in DGK inhibitor II-treated $Hdh^{111Q/111Q}$ cells after serum withdrawal was not altered by PKC inhibitors bisindolylmaleimide I (*BIM1*) or Gö6983. After seeding, $Hdh^{111Q/111Q}$ cells were cultured in normal 10% FBS (column 1) or serum-free medium (*columns 2–5*) for 24 h. Dimethyl sulfoxide (*DMSO*) control or 20 μM DGK inhibitor II with or without 1 μM bisindolylmaleimide I or 1 μM Gö6983 were added simultaneously with serum withdrawal. Caspase activity assay was performed after the treatment. *B*, increased WST-8 by DGK inhibitor II in $Hdh^{111Q/111Q}$ cells after serum withdrawal was not affected by PKC inhibitors. $Hdh^{111Q/111Q}$ cells were treated the same as in *A*, and WST-8 assay was used instead of caspase activity assay. One-way analysis of variance was used for statistical analysis for both *A* and *B* (*ns*, not significant). *C*, decreased Htt fragment in $Hdh^{111Q/111Q}$ cells after serum withdrawal by DGK inhibitor was not affected by PKC inhibitors shown by Western blotting. Serum-starved $Hdh^{111Q/111Q}$ cells were co-treated with 10 μM DGK inhibitor II (*DGKi*) with or without 1 μM bisindolylmaleimide I or 1 μM Gö6983. Western blot using the antibody Htt2166 against Htt was performed. *rel.*, relative.

and $Hdh^{111Q/111Q}$ cells with or without DGK inhibitor II using MRM-MS (see supplemental Table 1 for MRM transitions). As shown in Fig. 4*A*, the levels of PI (38:4) are distinct in the $Hdh^{7Q/7Q}$ and $Hdh^{111Q/111Q}$ cells. The level of PI (38:4), PIP (38:4), and PIP_2 (38:4) in $Hdh^{7Q/7Q}$ cells is 1.8-, 1.3- and 2.4-fold higher, respectively, when compared with $Hdh^{111Q/111Q}$ cells in resting cells. Thus, mutant Htt expression results in lower levels of polyphosphoinositides. Strikingly, cells undergoing serum withdrawal have increased levels of PIP (38:4) and PIP_2 (38:4) (Fig. 4*B*). Treatment with 20 μM DGK inhibitor II in $Hdh^{111Q/111Q}$ cells reduces the levels of PIP (38:4) and PIP_2 (38:4) to 44 and 54%, respectively (Fig. 4*B*).

To further analyze alterations in lipid metabolism, we also performed immunocytochemistry on $Hdh^{7Q/7Q}$ and $Hdh^{111Q/111Q}$ cells using a pan-lipid antibody that recognizes PIPs. As shown in Fig. 4*C*, we detected less PIP staining in $Hdh^{111Q/111Q}$ when compared with $Hdh^{7Q/7Q}$ cells. Furthermore, the levels of PIP increased during serum withdrawal and were reduced by DGK inhibitor II treatment (Fig. 4*C*).

Identification of DGKϵ as Therapeutic Target for HD—There are 10 DGK mammalian isoforms, and therefore it is possible that one or several of these family members are possible therapeutic targets of the DGK inhibitors in the context of HD toxicity. Five DGK isoforms, α, β, γ, ϵ, and ξ have been shown to be expressed in the brain (19). To identify the isoforms most abundant in the striatum, we used RT-qPCR to quantify the isoforms in this region of the brain. β, γ, ϵ, and ξ DGK isoforms were expressed in the striatum (Fig. 5). We then knocked down these four DGKs in striatal $Hdh^{111Q/111Q}$ cells individually with siRNA and performed the caspase activity assay after serum starvation. Only the siRNA specific to DGKϵ resulted in decreased caspase-3/7 activity, similar to treatment of DGK inhibitors (Fig. 6*A*, data not shown for other DGKs). We confirmed the knockdown of DGKϵ using RT-qPCR (Fig. 6*B*), and the level was similar in magnitude to that found for the reduction in caspase-3/7 activity (Fig. 6*A*).

We also investigated whether the levels of DGKϵ are altered in response to mutant Htt. RT-qPCR for DGKϵ showed that $Hdh^{111Q/111Q}$ cells have higher levels of DGKϵ than $Hdh^{7Q/7Q}$ cells (Fig. 6*C*), indicating that DGKϵ levels are increased in response to mutant Htt.

In Vivo Evidence for DGKϵ Reduction in Levels of DGK ϵ Homolog Improves Neuronal Function in Drosophila Model of HD—We next sought to validate this observation *in vivo*. We found that in the striatum of R6/2 HD transgenic mice, a HD mouse model with overexpression of N-terminal fragment of Htt containing ~120 polyglutamines, the levels of DGKϵ are higher than in the striatum of littermate control mice (Fig. 7*A*). These results suggest a specific role of DGKϵ in HD toxicity.

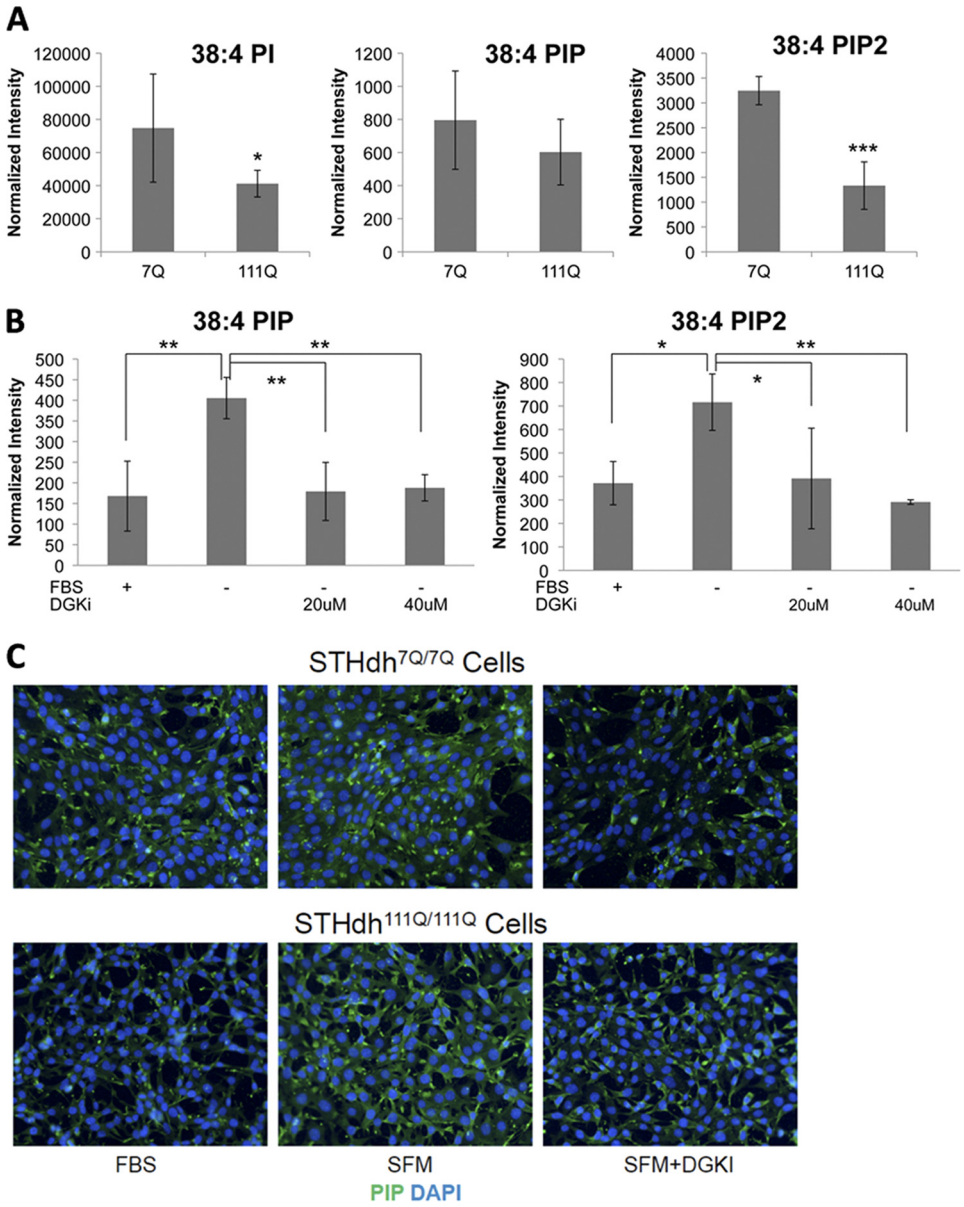

FIGURE 4. **Quantification of phosphoinositides in *Hdh*$^{7Q/7Q}$ *and Hdh*$^{111Q/111Q}$ cells using mass spectrometry.** *A*, *Hdh*$^{7Q/7Q}$ cells have higher levels of phosphoinositides (38:4) than *Hdh*$^{111Q/111Q}$ cells. Total lipids were collected from either *Hdh*$^{7Q/7Q}$ or *Hdh*$^{111Q/111Q}$ cells grown in normal 10% FBS condition. Lipid samples were subjected to MRM-MS for quantification. Intensities of each lipid species was normalized against cell numbers. *B*, in *Hdh*$^{111Q/111Q}$ cells serum deprivation caused increase in 38:4 PIP and PIP_2, whereas DGK inhibitor II blocked this increase. *Hdh*$^{111Q/111Q}$ cells were treated with serum-free medium with or without indicated concentration of DGK inhibitor II (*DGKi*) for 24 h before total lipid extraction. All samples were subjected to MRM-MS for quantification. Intensities of each lipid species were normalized against cell number. One-way analysis of variance was used for statistical analysis. *C*, immunocytochemistry of *Hdh*$^{7Q/7Q}$ and *Hdh*$^{111Q/111Q}$ cells using a pan-PIP antibody. Cells were subjected to 24 h serum-free medium treatment (*SFM*) in the presence or absence of 20 μM DGK inhibitor II. Images are at 20× magnification

The above data suggest that DGKϵ is involved in HD and may function as a suppressor of Htt-induced toxicity *in vivo*. To investigate this possibility, we studied the effect of decreasing DGKϵ levels in a well established *Drosophila* HD model (16). Expression of N-terminal Htt with a 128Q (*NT-Htt128Q*) expansion in the *Drosophila* nervous system (using the neuronal *elav-GAL4* driver) leads to progressive motor performance deficits when compared with normal animals (Fig. 7*B*, compare *blue* discontinuous line with *black dotted lines*). Consistent with *Hdh*$^{111Q/111Q}$ cell data, decreasing the levels of the *Drosophila* DGKϵ in the nervous system by means of an inducible shRNA line (*NT-Htt128Q*/*DGKϵ*^{shRNA} *4659GD*), significantly ameliorates the toxic effects of expanded Htt (Fig. 7*B*, compare *solid red lines* with *black dotted lines*). *NT-Htt128Q*/*DGKϵ*^{shRNA} *4659GD* show a delay in disease onset, and they perform better than animals expressing *NT-Htt128Q* with normal levels of DGKϵ. These data, together with the observation in the striatum of R6/2 mice, confirm that the Htt-DGKϵ interaction is relevant *in vivo*.

DISCUSSION

To identify new therapeutic targets in HD, we screened a kinase inhibitor library for molecules that block mutant Htt cellular toxicity. We found that DGK inhibitor II decreased caspase-3/7

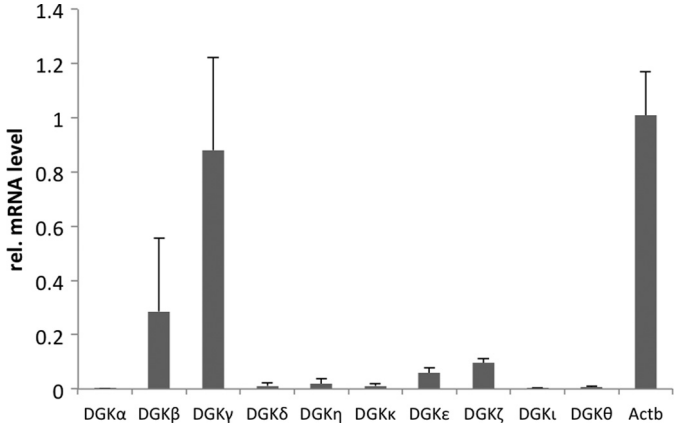

FIGURE 5. **Expression of DGK isoforms in mouse striatum.** Total RNA sample from mouse striatum tissue was subjected to RT-qPCR for all 10 mammalian DGK isoforms. Actb stands for β-actin, a housekeeping gene that we used for normalization. β, γ, ϵ, and ξ DGKs showed relatively higher expression levels. *rel.*, relative.

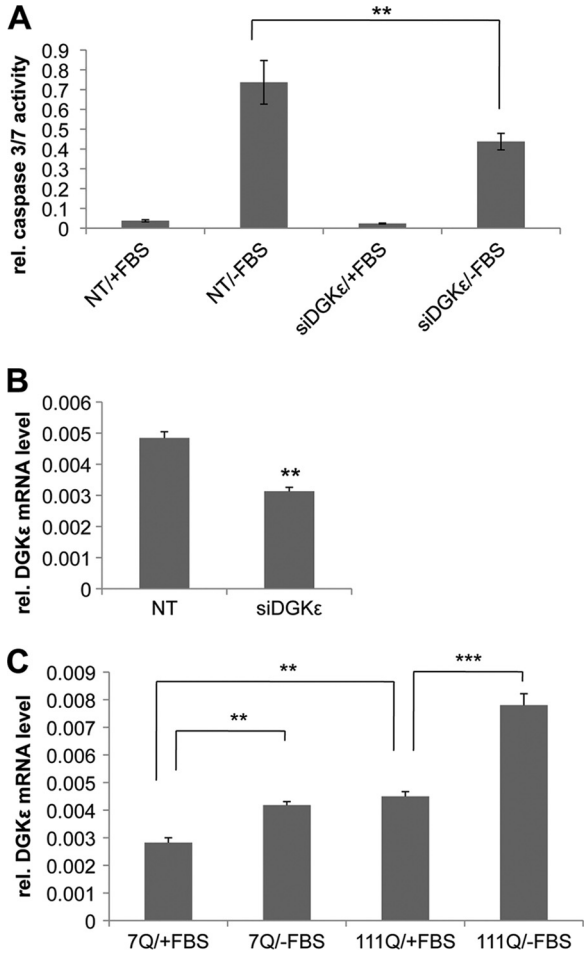

FIGURE 6. **DGKε in immortalized *Hdh*$^{111Q/111Q}$ cells.** *A*, DGKε was knocked down by siRNA in *Hdh*$^{111Q/111Q}$ cells before serum withdrawal. Caspase activity showed decreased levels of caspase-3/7 activity with siRNA specific to DGKε (siDGKε) compared with non-targeting (*NT*) siRNA in serum-starved *Hdh*$^{111Q/111Q}$ cells. *B*, RT-qPCR confirmed knockdown of DGKε in *Hdh*$^{111Q/111Q}$ cells. Student's *t* test was used for statistical analysis. *C*, RT-qPCR showed higher expression level of DGKε in *Hdh*$^{111Q/111Q}$ cells than in normal *Hdh*$^{7Q/7Q}$ cells. Serum starvation further increased DGKε expression. One-way analysis of variance was used for statistical analysis. *rel.*, relative.

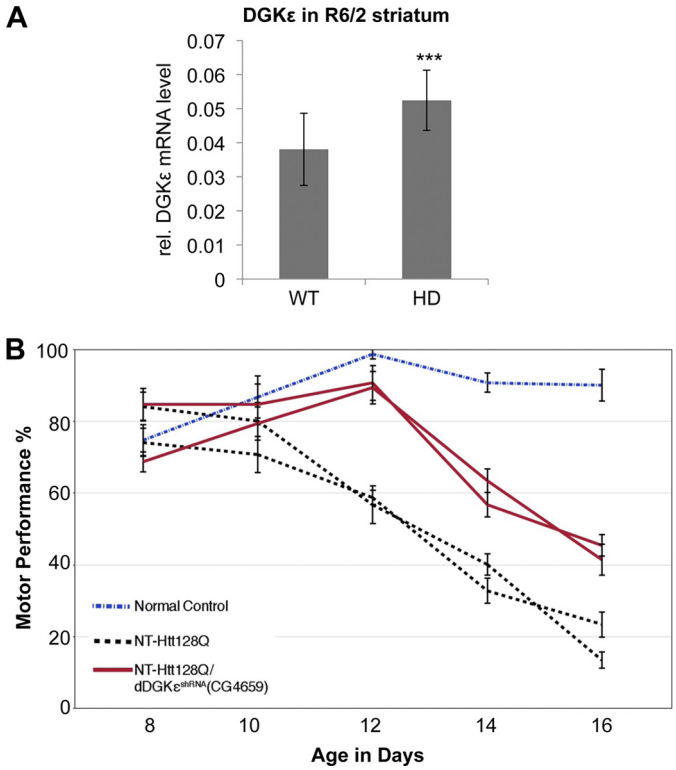

FIGURE 7. **DGKε in mouse and *Drosophila* HD models.** *A*, RT-qPCR showed higher DGKε level in transgenic HD R6/2 striatum than in wild type (WT) mouse striatum tissue at the age of 10.5 weeks (Student's *t* test, $p < 0.001$). *B*, reduction in DGKε homolog improves neuronal function in a *Drosophila* model of HD. Chart represents motor performance as a function of age in control flies and flies expressing NT-Htt128Q either alone or together with an inducible shRNA targeting the *Drosophila* DGKε homolog (CG8657), in the nervous system. Test measures the ability of the animals to climb 9.5 cm in 15 s (see "Experimental Procedures" for details). Control animals (*blue dashed line*) perform well in the motor performance test for the complete duration of the experiment. Animals expressing NT-Htt128Q in the nervous system show progressive impairment of motor performance starting at day 12 (*black dotted line*). Animals expressing NT-Htt128Q in the nervous system together with an shRNA targeting the *Drosophila* DGKε homolog show a suppression of the Htt-induced motor performance impairment (*solid red lines*). Notice that the Htt128Q/DGKε^{shRNA} 4659GD animals show delayed disease onset (impairments begin at day 14) and continue to perform better than the NT-Htt128Q for the remainder of the experiment. Genotypes are as follows: *normal control*, Elav-GAL4/w1118; *NT-Htt128Q*, Elav-GAL4/w1118;+;UAS-NT-Htt128Q(f33A)/+. *Htt128Q/DGKε^{shRNA}*4659GD: Elav-GAL4/w1118; DGKε^{shRNA}4659GD/+;UAS-NT-Htt128Q(f33A)/+. *Error bars* represent S.E. Two experimental replicates are shown for the NT-Htt128Q and the Htt128Q/DGKε^{shRNA} animals.

activity after serum withdrawal in striatal *Hdh*$^{111Q/111Q}$ cells. Our screen also identified rapamycin as a kinase inhibitor that blocked mutant Htt-mediated cell death. The DGK inhibitor II decreased the level of cleaved caspase-3, the accumulation of the 513-amino acid N-terminal Htt fragment processed by caspase-3, and blocked alterations in lipid metabolism during serum withdrawal. We also tested the DGK inhibitor I, which was not in the initial library of 80 compounds, and this compound was effective as well.

There are 10 distinct mammalian isoforms of DGKs. To identify the possible diacylglycerol kinase family member that was responsible for rescuing striatal *Hdh*$^{111Q/111Q}$-mediated toxicity, we knocked down all four DGK isoforms expressed in the brain (β, γ, ϵ, and ζ) using siRNA. Only the knockdown of the family member, DGKε, blocked striatal *Hdh*$^{111Q/111Q}$-me-

diated toxicity. This isoform DGKϵ is unique in that it has a hydrophobic domain that facilitates attachment to membranes (20), and furthermore, it has specificity for diacylglycerol containing arachidonyl chains (21, 22). Loss of function of the *Drosophila* DGKϵ homolog was evaluated in an HD *Drosophila* model, and we found significant improvement of Htt-induced motor dysfunction. In addition, the levels of DGKϵ were higher in the striatum of R6/2 HD transgenic mice when compared with controls, confirming the relevance of the interaction *in vivo*.

We have discovered that inhibition of the enzyme DGK is protective to immortalized striatal cells expressing mutant Htt. Because the enzymatic activity of this protein is to catalyze the phosphorylation of DAG into PA, we expect that inhibition would lead to a rise in DAG production and decreased PA production. Classically, DGKs are known as regulators of PKC family members. However, we tested PKCs inhibitors and did not find the protection imparted by DGK inhibition was dependent upon PKCs for mutant Htt toxicity.

Because generation of PA through DAG phosphorylation also is the first step in PI resynthesis, we evaluated whether the inhibition of DGK could impact lipid metabolism in $Hdh^{7Q/7Q}$ and $Hdh^{111Q/111Q}$ cells. First, we found that the levels of PI, PIP, and PIP_2 in $Hdh^{7Q/7Q}$ cells are higher when compared with $Hdh^{111Q/111Q}$ cells. It is possible that the lower levels of PIs in the $Hdh^{111Q/111Q}$ cells reflect a compensatory mechanism to block striatal cell death. Consistent with this notion, we found that both $Hdh^{7Q/7Q}$ and $Hdh^{111Q/111Q}$ cells undergoing serum withdrawal had elevated levels of PIs. When we evaluated the impact of DGK inhibition on lipid levels in $Hdh^{111Q/111Q}$ cells undergoing serum withdrawal, we found the levels of PIP and PIP_2 were reduced significantly. In addition, immunocytochemistry demonstrated an increase in PIP signaling during serum withdrawal, which was blocked by DGK inhibition. This may be relevant to the protective effect of DGK inhibition.

A number of alterations in lipid metabolism have been noted before in HD. This includes lower cholesterol levels in affected areas of the brain (23) and reduced ganglioside (GM1) synthesis (24). Further modulation of GM1 restores normal motor behavior in HD mouse model YAC128 (25). Our findings further emphasize the role of altered lipid metabolism in HD, particularly with respect to phosphatidylinositols, which are already known to have distinct binding to the mutant Htt protein. This may be particularly important as the normal function of Htt appears to be involved in vesicular trafficking, and many protein complexes involved in this process require PIPs. Htt binds different forms of PIPs, whereas the mutant Htt bound to a subset of PIPs more strongly than wild type Htt in vesicle-binding assays (9). Therefore, inhibition of DGKs may alter the interaction of mutant Htt with PIPs.

DGKϵ levels as measured by RT-qPCR appear to be modulated by polyglutamine expansion in the Htt protein. We found higher levels of DGKϵ in immortalized striatal cells expressing mutant Htt and in the mouse model of R6/2 HD transgenic mouse model. Furthermore, cells undergoing cell death had increased levels of DGKϵ. This may increase the levels of PIP_2, which is known to regulate cell death through P2X7 receptors (26).

In conclusion, we have identified DGKϵ as a therapeutic target for HD. We have shown that pharmacological inhibition of DGK activity can improve Htt-induced toxicity in cells. In addition, we show that the abnormal phospholipid levels induced by mutant Htt are restored upon decreasing DGK activity. Finally, we also have observed *in vivo* that DGKϵ levels are increased in response to Htt and that decreasing DGKϵ levels rescues Htt toxicity in an animal model. There are DGKϵ mutant mice available (7, 8), and our future work will be aimed at how modulation of this enzyme in mammalians affects disease progression and neuropathology in HD mouse models.

Acknowledgment—Striatal $Hdh^{7Q/7Q}$ and $Hdh^{111Q/111Q}$ cells were provided generously by Dr. Marcy MacDonald (Massachusetts General Hospital).

REFERENCES

1. The Huntington's Collaborative Research Group (1993) A novel gene containing a trinucleotide repeat that is expanded and unstable on Huntington disease chromosomes. The Huntington Disease Collaborative Research Group. *Cell* **72,** 971–983
2. Mérida, I., Avila-Flores, A., and Merino, E. (2008) Diacylglycerol kinases: At the hub of cell signaling. *Biochem. J.* **409,** 1–18
3. Weissmann, N., Dietrich, A., Fuchs, B., Kalwa, H., Ay, M., Dumitrascu, R., Olschewski, A., Storch, U., Mederos y Schnitzler, M., Ghofrani, H. A., Schermuly, R. T., Pinkenburg, O., Seeger, W., Grimminger, F., and Gudermann, T. (2006) Classical transient receptor potential channel 6 (TRPC6) is essential for hypoxic pulmonary vasoconstriction and alveolar gas exchange. *Proc. Natl. Acad. Sci. U.S.A.* **103,** 19093–19098
4. Sakane, F., Imai, S., Kai, M., Yasuda, S., and Kanoh, H. (2007) Diacylglycerol kinases: Why so many of them? *Biochim. Biophys. Acta* **1771,** 793–806
5. Wu, J., Shih, H. P., Vigont, V., Hrdlicka, L., Diggins, L., Singh, C., Mahoney, M., Chesworth, R., Shapiro, G., Zimina, O., Chen, X., Wu, Q., Glushankova, L., Ahlijanian, M., Koenig, G., Mozhayeva, G. N., Kaznacheyeva, E., and Bezprozvanny, I. (2011) Neuronal store-operated calcium entry pathway as a novel therapeutic target for Huntington disease treatment. *Chem. Biol.* **18,** 777–793
6. Lung, M., Shulga, Y. V., Ivanova, P. T., Myers, D. S., Milne, S. B., Brown, H. A., Topham, M. K., and Epand, R. M. (2009) Diacylglycerol kinase epsilon is selective for both acyl chains of phosphatidic acid or diacylglycerol. *J. Biol. Chem.* **284,** 31062–31073
7. Rodriguez de Turco, E. B., Tang, W., Topham, M. K., Sakane, F., Marcheselli, V. L., Chen, C., Taketomi, A., Prescott, S. M., and Bazan, N. G. (2001) Diacylglycerol kinase epsilon regulates seizure susceptibility and long-term potentiation through arachidonoyl-inositol lipid signaling. *Proc. Natl. Acad. Sci. U.S.A.* **98,** 4740–4745
8. Milne, S. B., Ivanova, P. T., Armstrong, M. D., Myers, D. S., Lubarda, J., Shulga, Y. V., Topham, M. K., Brown, H. A., and Epand, R. M. (2008) Dramatic differences in the roles in lipid metabolism of two isoforms of diacylglycerol kinase. *Biochemistry* **47,** 9372–9379
9. Kegel, K. B., Sapp, E., Alexander, J., Valencia, A., Reeves, P., Li, X., Masso, N., Sobin, L., Aronin, N., and DiFiglia, M. (2009) Polyglutamine expansion in huntingtin alters its interaction with phospholipids. *J. Neurochem.* **110,** 1585–1597
10. Tang, T. S., Tu, H., Chan, E. Y., Maximov, A., Wang, Z., Wellington, C. L., Hayden, M. R., and Bezprozvanny, I. (2003) Huntingtin and huntingtin-associated protein 1 influence neuronal calcium signaling mediated by inositol (1,4,5)-triphosphate receptor type 1. *Neuron* **39,** 227–239
11. Tang, T. S., Guo, C., Wang, H., Chen, X., and Bezprozvanny, I. (2009) Neuroprotective effects of inositol 1,4,5-trisphosphate receptor C-terminal fragment in a Huntington disease mouse model. *J. Neurosci.* **29,** 1257–1266
12. Trettel, F., Rigamonti, D., Hilditch-Maguire, P., Wheeler, V. C., Sharp,

A. H., Persichetti, F., Cattaneo, E., and MacDonald, M. E. (2000) Dominant phenotypes produced by the HD mutation in STHdh(Q111) striatal cells. *Hum. Mol. Genet.* **9,** 2799–2809
13. Leyva, M. J., Degiacomo, F., Kaltenbach, L. S., Holcomb, J., Zhang, N., Gafni, J., Park, H., Lo, D. C., Salvesen, G. S., Ellerby, L. M., and Ellman, J. A. (2010) Identification and evaluation of small molecule pan-caspase inhibitors in Huntington disease models. *Chem. Biol.* **17,** 1189–1200
14. Kim, Y., Shanta, S. R., Zhou, L. H., and Kim, K. P. (2010) Mass spectrometry-based cellular phosphoinositides profiling and phospholipid analysis: A brief review. *Exp. Mol. Med.* **42,** 1–11
15. Wenk, M. R., Lucast, L., Di Paolo, G., Romanelli, A. J., Suchy, S. F., Nussbaum, R. L., Cline, G. W., Shulman, G. I., McMurray, W., and De Camilli, P. (2003) Phosphoinositide profiling in complex lipid mixtures using electrospray ionization mass spectrometry. *Nat. Biotechnol.* **21,** 813–817
16. Al-Ramahi, I., Lam, Y. C., Chen, H. K., de Gouyon, B., Zhang, M., Pérez, A. M., Branco, J., de Haro, M., Patterson, C., Zoghbi, H. Y., and Botas, J. (2006) CHIP protects from the neurotoxicity of expanded and wild-type ataxin-1 and promotes their ubiquitination and degradation. *J. Biol. Chem.* **281,** 26714–26724
17. Miller, J. P., Holcomb, J., Al-Ramahi, I., de Haro, M., Gafni, J., Zhang, N., Kim, E., Sanhueza, M., Torcassi, C., Kwak, S., Botas, J., Hughes, R. E., and Ellerby, L. M. (2010) Matrix metalloproteinases are modifiers of huntingtin proteolysis and toxicity in Huntington's disease. *Neuron* **67,** 199–212
18. Ravikumar, B., Vacher, C., Berger, Z., Davies, J. E., Luo, S., Oroz, L. G., Scaravilli, F., Easton, D. F., Duden, R., O'Kane, C. J., and Rubinsztein, D. C. (2004) Inhibition of mTOR induces autophagy and reduces toxicity of polyglutamine expansions in fly and mouse models of Huntington disease. *Nat. Genet.* **36,** 585–595
19. Goto, K., and Kondo, H. (1999) Diacylglycerol kinase in the central nervous system–molecular heterogeneity and gene expression. *Chem. Phys. Lipids* **98,** 109–117
20. Dicu, A. O., Topham, M. K., Ottaway, L., and Epand, R. M. (2007) Role of the hydrophobic segment of diacylglycerol kinase epsilon. *Biochemistry* **46,** 6109–6117
21. Walsh, J. P., Suen, R., Lemaitre, R. N., and Glomset, J. A. (1994) Arachidonoyl-diacylglycerol kinase from bovine testis. Purification and properties. *J. Biol. Chem.* **269,** 21155–21164
22. Tang, W., Bunting, M., Zimmerman, G. A., McIntyre, T. M., and Prescott, S. M. (1996) Molecular cloning of a novel human diacylglycerol kinase highly selective for arachidonate-containing substrates. *J. Biol. Chem.* **271,** 10237–10241
23. Valenza, M., and Cattaneo, E. (2011) Emerging roles for cholesterol in Huntington disease. *Trends Neurosci.* **34,** 474–486
24. Maglione, V., Marchi, P., Di Pardo, A., Lingrell, S., Horkey, M., Tidmarsh, E., and Sipione, S. (2010) Impaired ganglioside metabolism in Huntington disease and neuroprotective role of GM1. *J. Neurosci.* **30,** 4072–4080
25. Di Pardo, A., Maglione, V., Alpaugh, M., Horkey, M., Atwal, R. S., Sassone, J., Ciammola, A., Steffan, J. S., Fouad, K., Truant, R., and Sipione, S. (2012) Ganglioside GM1 induces phosphorylation of mutant huntingtin and restores normal motor behavior in Huntington disease mice. *Proc. Natl. Acad. Sci. U.S.A.* **109,** 3528–3533
26. Zhao, Q., Yang, M., Ting, A. T., and Logothetis, D. E. (2007) PIP_2 regulates the ionic current of P2X receptors and P2X7 receptor-mediated cell death. *Channels* **1,** 46–55